

Schottky-barrier double-walled carbon nanotube field-effect transistors

Shidong Wang and Milena Grifoni

Theoretische Physik, Universität Regensburg, 93040 Regensburg, Germany.

(Dated: February 8, 2020)

We investigate electronic transport properties of Schottky-barrier field-effect transistors (FET) based on double-walled carbon nanotubes (DWNT) with a semiconducting outer shell and a metallic inner one. These kind of DWNT-FETs show asymmetries of the I - V characteristics and threshold voltages due to the electron-hole asymmetry of the Schottky barrier. The presence of the metallic inner shell induces a large effective band gap, which is one order of magnitude larger than that due to the semiconducting shell alone of a single-walled carbon nanotube FET.

PACS numbers: 73.63.Fg, 85.35.Kt, 73.40.Cg

Due to their special electronic and mechanic properties, carbon nanotubes have become promising building blocks for fundamental nanoscale devices, such as field-effect transistors (FET)^{1,2}. Carbon nanotubes can be either single-walled (SWNT), double-walled (DWNT) or multi-walled (MWNT), depending on whether they consist of one, two or several graphene sheets wrapped onto concentric cylinders. Early attempt to fabricate room-temperature MWNT-FETs was not successful because of the large MWNT radii (about 10 nm) such that the band gap is comparable with the thermal energy at room temperature³. Hence, experimental and theoretical investigations mainly focussed on FETs based on semiconducting SWNTs^{3,4,5,6,7,8,9,10,11,12}. A SWNTs is characterized by so-called chiral indices (n, m) and whether it is metallic or semiconducting is solely determined by the chiral indices¹. These devices show many different properties than the traditional bulk counterparts, due to the cylindrical shape and the one-dimensional character of the electronic band structure of SWNTs. For example, the lack of Fermi-level pinning¹², which plays an important role for the contact properties of bulk FETs, makes it possible to control the height of Schottky barriers in SWNT-FETs by using metals with different work functions. SWNT-FETs without Schottky barriers have already been demonstrated⁷. The effects of a Schottky barrier have been investigated both theoretically and experimentally in^{6,9,10,11}. As the band gap in a semiconducting SWNT is inversely proportional to the tube radius¹, FETs with different band gaps can be fabricated by using nanotubes with different radii. FETs based on SWNTs with small radii can be either p or n -type¹³. Devices based on nanotubes with large radius exhibit ambipolar behavior^{3,14}.

Properties of FETs based on DWNTs have not been fully explored yet. In the last two years, DWNT-FETs have been fabricated^{15,16,17,18}. Due to their larger radii, DWNT-FETs usually exhibit ambipolar behavior^{15,16,17}. So far, three distinct types of field-effect characteristics have been observed. These were attributed to the possibility of having semiconducting and/or metallic inner and outer shells. In particular, of the devices which show FET behavior at low temperatures, only a part also shows such behavior at high temperatures¹⁸, which

may be due to the presence of an inner metallic shell. In fact, it has been shown that the intershell coupling strongly depends on the energy and commensurability of two shells. For incommensurate DWNT, at low energies, the intershell coupling is negligible^{19,20,21,22}, while it becomes quite large at high energies^{20,23,24}. FET behaviors are thus destroyed at high temperatures because the metallic inner shell can accommodate electrons which screen the outer shell. By using a two-ladder model for a DWNT with a semiconducting outer shell, a metallic inner one and a large intershell coupling, it was shown in Ref.²⁵ that the intershell coupling can induce a finite density of states in the band gap of the outer shell, which destroys the FET behavior. Because of the assumption of a large intershell coupling, the conclusions in Ref.²⁵ are valid at high temperatures only. The same devices show FET behavior at low temperatures¹⁸, which indicates that the intershell coupling becomes negligible at low temperatures. The effects of the metallic inner shell on the device properties at low temperatures, being object of this work, have not been evaluated so far.

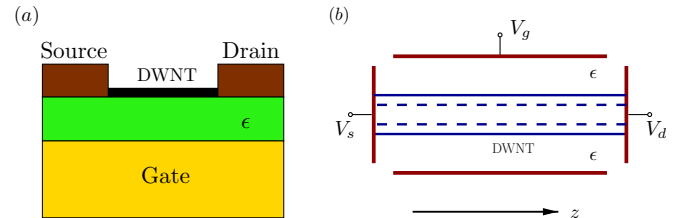


FIG. 1: (color online) (a) Schematic experimental setup of a double-walled carbon nanotube (DWNT) field-effect transistor (FET). A DWNT is connected with source and drain contacts. A gate is insulated from the DWNT by a dielectric material with dielectric constant ϵ . (b) A theoretical model describing the setup in (a). The FET consists of a DWNT with a semiconducting outer shell and a metallic inner one. Only the outer shell is “end-bonded” to the source and drain contacts and the inner one is insulated from both leads. A cylindrical gate is deposited on the dielectric material surrounding the DWNT.

Specifically, we investigate the electronic transport properties of a FET based on a DWNT with a semiconducting outer shell and an incommensurate metallic

inner one at low temperatures ($\ll \Delta E$, where ΔE is the gap between neighboring subbands), in which case the intershell coupling can be neglected. As shown in previous works^{19,20,21}, the intershell coupling is negligible at low temperatures for incommensurate shells. Moreover, most semiconducting-metallic DWNTs are incommensurate. Within a model which incorporates a coaxial gate, the outer shell connecting to bulk electrodes and a metallic inner shell, we show that a Schottky barrier arises. Electron-hole asymmetry of the Schottky barrier causes the asymmetries of the I - V characteristics and threshold voltages. We also show that the existence of the metallic inner shell induces a very large effective band gap, which makes it possible to fabricate workable FETs based on DWNTs with quite large radii.

A schematic experimental setup of a DWNT-FET is shown in Fig. 1(a). A DWNT is contacted with source and drain electrodes and a planar gate is situated underneath a dielectric layer with dielectric constant ϵ . The model describing the device is schematically shown in Fig. 1(b). The DWNT consists of a semiconducting outer shell and a metallic inner one. Experimentally, the metallic electrodes are typically evaporated on top of the outer shell. Hence we assume that the outer shell only is “end-bonded” with source and drain leads. As the shape of the gate does not change the FET characteristics qualitatively¹⁰, to simplify the calculations we consider a cylindrical gate deposited on a dielectric material with dielectric constant ϵ surrounding the DWNT. As we focus on low temperatures, we only include the lowest valence and conduction bands of both shells. We assume zero intershell coupling and a ratio between the length and the circumference much larger than one. Hence, as shown in Ref.²⁶, we can assume an equipotential surface of the metallic inner shell. The potential value V_i is related to the doping on the inner shell, which depends on the preparation conditions of the DWNT. Hence the inner shell acts effectively as another gate. We treat V_i as a parameter in the following calculations. The device possesses azimuthal symmetry, and hence the electrostatic potential felt by the electrons in the device, $\varphi(z, \rho)$, depends only on the longitudinal coordinate z and on the distance ρ from the nanotube axis. It can be calculated by the Laplace equation in cylindrical coordinates,

$$\frac{\partial^2 \varphi(z, \rho)}{\partial \rho^2} + \frac{1}{\rho} \frac{\partial \varphi(z, \rho)}{\partial \rho} + \frac{\partial^2 \varphi(z, \rho)}{\partial z^2} = 0 \quad (1)$$

with the boundary condition on the surface of the semiconducting outer shell, $(\epsilon \nabla \psi - \epsilon_0 \nabla \psi) \cdot \mathbf{n} = -Q(z)$, where \mathbf{n} is a unit normal to the surface and we assume that the dielectric constant between two shells is the same as that of the air, ϵ_0 . The charge density on the surface is $Q(z) = q(z)/2\pi R_o$ with R_o the radius of the outer shell and $q(z)$ the charge density on it. We set the source voltage as the reference potential, that is, $V_s = 0$. Then the boundary conditions are specified by the drain voltage V_d , the gate voltage V_g and the potential on the inner

shell V_i as

$$\begin{aligned} \varphi(0, \rho) &= -\Delta W/e, & \varphi(z, D_g + R_o) &= V_g, \\ \varphi(L, \rho) &= V_d - \Delta W/e, & \varphi(z, R_i) &= V_i, \end{aligned}$$

where e is the elementary charge and ΔW is the difference between the work function of leads and the affinity of the semiconducting shell. The length of the DWNT is L , R_i is the radius of the inner shell and D_g is the thickness of the dielectric material. We consider low transparency of the barrier such that carriers in the DWNT are described by the Fermi-Dirac distribution also for finite bias. Without loss of generality we assume that the outer shell is not heavily doped so that it is an intrinsic semiconductor. Hence, the charge density $q(z)$ on the outer shell can be calculated as

$$q(z) = -e \int dE (\nu_e(E, z) f_e(E - \mu_o) - \nu_h(E, z) f_h(E - \mu_o)). \quad (2)$$

Here $f_e(E - \mu_o) = 1/(1 + \exp((E - \mu_o)/k_B T))$ is the Fermi distribution function with the temperature T and the chemical potential μ_o in the outer shell. The distribution function of holes is $f_h(E) = 1 - f_e(E)$. Finally, $\nu_e(E)$ and $\nu_h(E)$ are the densities of states (DOS) of electrons and holes in the semiconducting shell, respectively. The lengths of DWNTs used in FET devices are usually about hundreds of nanometers and hence are much smaller than the charge mean free path²⁰. Therefore, we assume ballistic transport of both electrons and holes in the outer shell. The chemical potential is then given by $\mu_o = -eV_d/2$. By using a tight-binding model for p_z electrons in DWNTs¹, with Fermi velocity $v_F = 8.5 \times 10^5$ m/s, intrashell coupling $\gamma_0 \approx 2.7$ eV and the carbon bond length $a_0 \approx 0.14$ nm¹, the DOS of electrons and holes is then given by

$$\begin{aligned} \nu_e(E, z) &= \frac{4}{\pi \hbar v_F} \frac{|E - E_c(z) + \Delta| \Theta(E - E_c)}{\sqrt{(E - E_c(z) + \Delta)^2 - \Delta^2}}, \\ \nu_h(E, z) &= \frac{4}{\pi \hbar v_F} \frac{|E - E_v(z) - \Delta| \Theta(-E + E_v)}{\sqrt{(E - E_v(z) - \Delta)^2 - \Delta^2}}, \end{aligned}$$

with the step function $\Theta(E)$. The gap between valence and conduction bands is $2\Delta = \gamma_0 a_0 / R_o$. The conduction and valence band edges are given as $E_c(z) = -e\varphi(z, R_o)$ and $E_v(z) = -e\varphi(z, R_o) - 2\Delta$. We solve the equations Eq. (1) and Eq. (2) self-consistently to obtain the electrostatic potential $\varphi(z, \rho)$.

Under our assumption of ballistic transport, we use the Landauer formula to calculate the currents of both electrons and holes, which are given as

$$\begin{aligned} I_e &= \frac{4e}{h} \int dE \Theta(E - E_c^m) T_e(E) (f_e(E) - f_e(E + eV_d)), \\ I_h &= \frac{4e}{h} \int dE \Theta(-E + E_v^M) T_h(E) (f_h(E) - f_h(E + eV_d)), \end{aligned}$$

where $T_e(E)$ and $T_h(E)$ are transmission coefficients of electrons and holes, respectively. $E_c^m = \min(E_c(z))$ and

$E_v^M = \max(E_v(z))$ are the minimum of the conduction band edge and the maximum of the valence band edge, respectively. The total current through the device is

$$I = I_h - I_e.$$

There are two contributions to the total transmission of the charges. One is due to the contact barriers and the other is due to the Schottky barrier. We assume that the transmission coefficient due to the contact is very small, $T_c \ll 1$ ($T_c \sim 10^{-3}$ to yield currents observed in Refs.¹⁷ and¹⁸). The total transmission coefficients for electrons and holes can be then calculated by using the WKB approximation and are given by

$$\begin{aligned} T_e(E) &= T_c \exp\left(-\frac{2}{\hbar} \left| \int dz \sqrt{2m_e(E - E_c(z))} \right| \right), \\ T_h(E) &= T_c \exp\left(-\frac{2}{\hbar} \left| \int dz \sqrt{2m_h(-E + E_v(z))} \right| \right), \end{aligned} \quad (3)$$

where $m_e = m_h = 2\hbar^2/9\gamma_0 a_0 R_o$ are effective masses of electrons and holes, respectively and T_c is the transmission coefficient due to the contacts. The integrations are performed in the classical forbidden regions for electrons and holes, respectively, for a fixed energy E . We set the transmission coefficients to be one if there are no classical forbidden regions.

In the calculations, we choose a 200 nm-long DWNT with outer shell radius $R_o = 1.34$ nm and inner shell radius $R_i = 1.0$ nm. The thickness of the dielectric material is $D_g = 22.78$ nm and its dielectric constant $\epsilon = 3.9\epsilon_0$ (as for SiO_2). The band gap of the semiconducting outer shell is 0.38 V corresponding to a (35, 0) shell. We assume that there is no doping in the DWNT and the chemical potential of the outer shell is at the mid-gap when there are no applied bias and gate voltages. We also choose that the difference between work function of leads and the affinity of electrons in the outer shell is $\Delta W = 0.19$ eV, which is the height of the Schottky barrier for both electron and hole when no bias and gate voltages is applied. The bias voltage is $V_{sd} = -V_d$, where the source voltage is grounded. The calculated I - V_{sd} characteristics with different gate voltages V_g at zero temperature are shown in Fig. 2(a). Here, we assume that the inner shell potential is $V_i = 0$ V. Under positive bias voltage the total current is mostly contributed by the electron current while at negative bias voltage the hole current dominates. We find an electron-hole asymmetry of the I - V characteristics. The threshold voltages shift with gate voltages and the amount of threshold shifts has also electron-hole asymmetry. This can be explained by the electron-hole asymmetry of the Schottky barrier, as shown in Fig. 2(b) and (c). Similar asymmetries of I - V characteristics and threshold voltages have also been observed in SWNT devices^{9,27}.

Because the DOS in a metallic shell is much smaller than that in a semiconducting shell, the chemical potential of the inner metallic shell of a DWNT may be significantly changed by doping while the chemical potential of the semiconducting outer shell may be still at

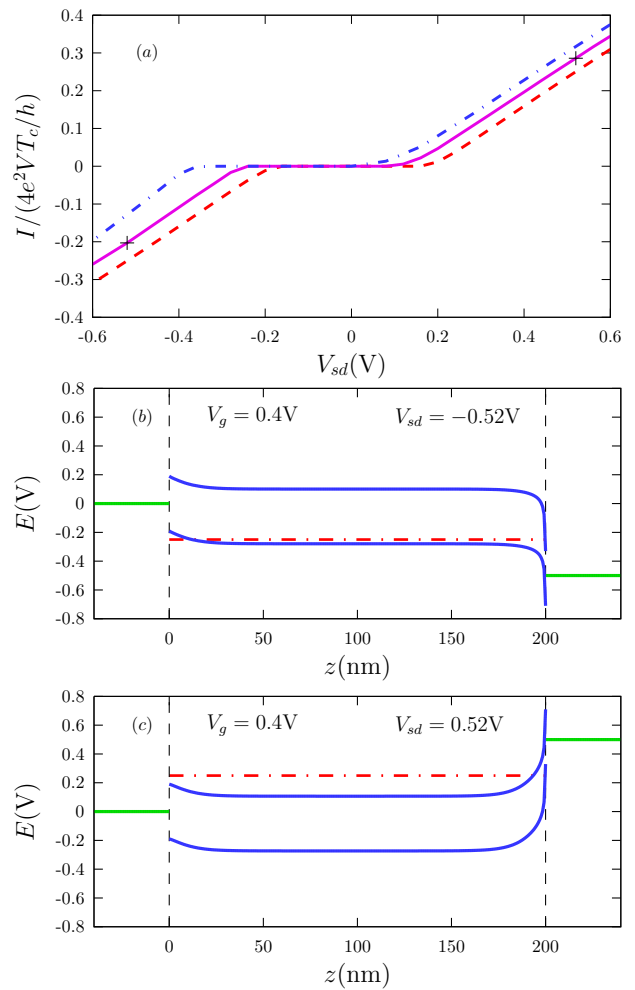


FIG. 2: (Color online) (a) Calculated zero temperature I - V_{sd} characteristics of a DWNT-FET with different gate voltages: $V_g = 0$ V (dashed line), $V_g = 0.4$ V (solid line), and $V_g = 0.8$ V (dot-dashed line). The DWNT has an outer shell with radius $R_o = 1.34$ nm and an inner one with radius $R_i = 1$ nm. Its length is $L = 200$ nm. The inner shell potential is $V_i = 0$ V. (b) and (c): Band diagrams of the conduction and valence band edges of the semiconducting outer shell in two configurations indicated by two crosses in (a). The dot-dashed line denotes the chemical potential in the outer shell. Two short thin solid lines show the chemical potentials in source (left) and drain (right) leads, respectively.

the mid-gap. Therefore, we consider the transfer characteristics of the same device with different inner shell potentials, as shown in Fig. 3. The bias voltage is fixed to be $V_{sd} = 0.05$ V. The inner shell potential only shifts the threshold gate voltages. The transfer characteristics of a SWNT-FET with the same radius as the DWNT outer shell, $R = 1.34$ nm, is shown in the inset of Fig. 3. Since the band gap of a semiconducting shell only depends on the radius, the SWNT has the same band gap as the outer DWNT shell. We find that the metallic inner shell has great influence on the transport properties of DWNT-FETs even if the intershell coupling vanishes.

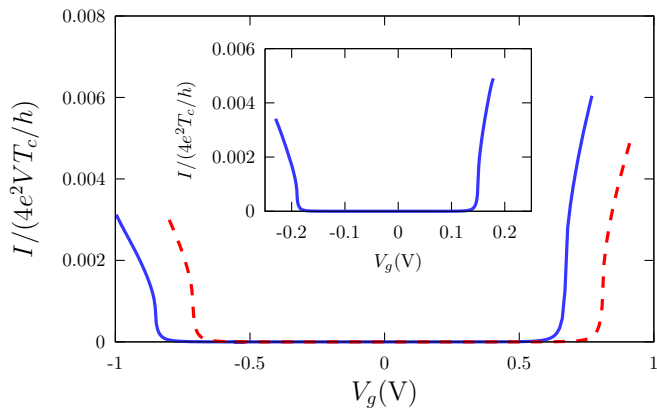


FIG. 3: (Color online) Transfer characteristics of a DWNT-FET with a constant bias voltage $V_{sd} = 0.05$ V but different inner shell potentials: $V_i = 0$ V (solid line) and $V_i = -0.04$ V (dashed line). The remaining parameters are the same as those in Fig. 2. Inset: Transfer characteristics of a SWNT-FET with radius $R = 1.34$ nm, which is the same as the outer shell radius of the DWNT.

The threshold gate voltages of the SWNT-FET are of the order of the band gap, but are one order of magnitude smaller than those of the DWNT-FET. Therefore, the DWNT-FETs behave like SWNT-FETs *with much smaller radius*, that is, with larger band gap. This is due to the existence of the metallic inner shell acting like another gate. Because the distance between the in-

ner and the outer shell (about 0.34 nm) is much smaller than that between outer shell and the gate (about tens of nanometers), the potential in the outer shell $\varphi(z, R_o)$ is almost “pinned” by the potential in the inner one V_i . As V_i is fixed, a very large change of V_g is needed in order to change a small amount of $\varphi(z, R_o)$. Therefore, the threshold gate voltages are much larger than the band gap. On the other hand, the potential in a SWNT is not “pinned” and can be varied quite easily by the gate voltage. Hence the threshold gate voltage in SWNT-FETs is of the same order of the band gap. We also expect that the threshold gate voltages in DWNT-FETs with two semiconducting shells are also of the same order of the band gap because the potential is not “pinned”.

In conclusion, we investigated electronic transport properties of FETs based on DWNTs with a semiconducting outer shell and a metallic inner one at low temperatures. DWNT-FETs shows asymmetries of the I - V characteristics and of threshold voltages due to the electron-hole asymmetric Schottky barrier. The potential of the outer shell is almost “pinned” by the potential of the inner one, which results in a large effective band gap of the outer shell. This latter fact can be of big relevance for carbon-nanotube based electronic devices.

Acknowledgments

The authors acknowledge the support of DFG under the program GRK 638.

-
- ¹ R. Saito, G. Dresselhaus, and M. S. Dresselhaus, *Physical Properties of Carbon Nanotubes* (Imperial College Press, London, 1998).
 - ² A. Graham, G. Duesberg, W. Hoenlein, F. Kreupl, M. Liebau, R. Martin, B. Rajasekharan, W. Pamler, R. Seidel, W. Steinhögl, et al., *Appl. Phys. A* **80**, 1141 (2005).
 - ³ R. Martel, T. Schmidt, H. Shea, T. Hertel, and P. Avouris, *Appl. Phys. Lett.* **73**, 2447 (1998).
 - ⁴ S. Tans, A. Verschueren, and C. Dekker, *Nature* **393**, 49 (1998).
 - ⁵ H. Postma, T. Teepen, Z. Yao, M. Grifoni, and C. Dekker, *Science* **293**, 76 (2001).
 - ⁶ S. Heinze, J. Tersoff, R. Martel, V. Derycke, J. Appenzeller, and P. Avouris, *Phys. Rev. Lett.* **89**, 106801 (2002).
 - ⁷ A. Javey, J. Guo, Q. Wang, M. Lundstrom, and H. Dai, *Nature* **424**, 654 (2003).
 - ⁸ F. Léonard and J. Tersoff, *Phys. Rev. Lett.* **83**, 5174 (1999).
 - ⁹ A. A. Odintsov, *Phys. Rev. Lett.* **85**, 150 (2000).
 - ¹⁰ T. Nakanishi, A. Bachtold, and C. Dekker, *Phys. Rev. B* **66**, 073307 (2002).
 - ¹¹ J. Appenzeller, J. Knoch, M. Radosavljevic, and P. Avouris, *Phys. Rev. Lett.* **92**, 226802 (2004).
 - ¹² F. Léonard and J. Tersoff, *Phys. Rev. Lett.* **84**, 4693 (2000).
 - ¹³ P. Avouris, *Acc. Chem. Res.* **35**, 1026 (2002).
 - ¹⁴ C. Zhou, J. Kong, and H. Dai, *Appl. Phys. Lett.* **76**, 1597 (2000).
 - ¹⁵ T. Shimada, T. Sugai, Y. Ohno, S. Kishimoto, T. Mizutani, H. Yoshida, T. Okazaki, and H. Shinohara, *Appl. Phys. Lett.* **84**, 2412 (2004).
 - ¹⁶ D. Kang, N. Park, J. Hyun, E. Bae, J. Ko, J. Kim, and W. Park, *Appl. Phys. Lett.* **86**, 93105 (2005).
 - ¹⁷ Y. Li, R. Hatakeyama, T. Kaneko, T. Izumida, T. Okada, and T. Kato, *Appl. Phys. Lett.* **89**, 93110 (2006).
 - ¹⁸ S. Wang, X. Liang, Q. Chen, Z. Zhang, and L. Peng, *J. Phys. Chem. B* **109**, 17361 (2005).
 - ¹⁹ Y.-G. Yoon, P. Delaney, and S. G. Louie, *Phys. Rev. B* **66**, 073407 (2002).
 - ²⁰ S. Wang and M. Grifoni, *Phys. Rev. Lett.* **95**, 266802 (2005).
 - ²¹ B. Bourlon, C. Miko, L. Forró, D.C. Glattli, and A. Bachtold, *Phys. Rev. Lett.* **93**, 176806 (2004).
 - ²² S. Uryu and T. Ando, *Phys. Rev. B* **72**, 245403 (2005).
 - ²³ S. Roche, F. Triozon, A. Rubio, and D. Mayou, *Phys. Rev. B* **64**, 121401(R) (2001).
 - ²⁴ S. Wang, M. Grifoni, and S. Roche, *Phys. Rev. B* **74**, 121407(R) (2006).
 - ²⁵ J. Lu, S. Yin, Z. Sun, X. Wang, and L. Peng, *Appl. Phys. Lett.* **90**, 052109 (2007).
 - ²⁶ A. Svizhenko and M. P. Anantram, *Phys. Rev. B* **72**, 085430 (2005).
 - ²⁷ Z. Yao, H. W. C. Postma, L. Balents, and C. Dekker, *Nature* **402**, 273 (1999).